Analytical Methods

ROYAL SOCIETY OF CHEMISTRY

PAPER

View Article Online
View Journal

Cite this: DOI: 10.1039/d6ay00400h

Rapid and targeted HILIC-MS/MS quantification of urinary metabolites reveals metabolic alterations in COVID-19 patients

Ondrej Hodek, *[ab] Anna Edman,[ab] Christoffer Granvik, [c] Alicia Lind,[de] Anna K. Överby,[cd] Mareike Gutensohn [bf] and Annika I. Johansson[bf]

Urinary metabolites and their concentrations serve as biomarkers for identification of metabolic pathways that relate to specific diseases; therefore, fast and accurate quantification of the metabolites in urine is essential in health assessment and diagnosis. As many urinary metabolites are of polar nature, hydrophilic interaction liquid chromatography (HILIC) has been used over the last several years because it offers faster and more reproducible analyses compared to traditional techniques such as reversed-phase chromatography or capillary electrophoresis. In our study, we developed a HILIC method by using a 3 cm analytical column in connection with tandem mass spectrometry detection for quantification of 10 urinary metabolites including creatinine as the reference for normalization. As all tested metabolites contain ionizable functional groups, pH of the mobile phase was optimized to achieve baseline separation of 2 isomeric pairs (1-methyl-4-imidazoleacetic acid/1-methyl-5-imidazoleacetic acid and 1-methylhistidine/3-methylhistidine) and to obtain overall better separation efficiency resulting in a 7 min analysis. The developed method was validated in terms of sensitivity, carry-over, linearity, matrix effects, accuracy, and precision. The metabolite concentrations in healthy subjects determined by the developed method correspond well with the normal reference values found in the literature. Moreover, the method was tested on a small cohort of COVID-19 patients, where it enabled identification of differences in metabolite levels. Thus, the developed method has potential to be used routinely in a diagnostic field for high-throughput analysis of urine samples.

Received 6th March 2026
Accepted 4th June 2026

DOI: 10.1039/d6ay00400h

rsc.li/methods

Introduction

Histamine, the most important mediator released from mast cells, plays a central role in immune regulation, inflammation, and allergic responses. Dysregulation of histamine release causes serious and sometimes life-threatening conditions such as anaphylaxis and mast cell activation syndrome (MCAS).[1] Dysregulation of mast cell function and histamine release has also been suggested to play a role in both acute coronavirus disease 2019 (COVID-19) and post-COVID conditions.[2,3] Clinical diagnosis of disorders characterized by histamine release remains challenging, with serial measurements of serum tryptase considered the gold standard. As histamine is rapidly metabolized in plasma, its urinary metabolites – such as 1-methylhistamine (1MH) and 1-methyl-4-imidazoleacetic acid (tele-MIAA) – serve as stable markers of systemic histamine turnover and mast cell activation.[4] In particular, the degradation metabolite 1-methyl-4-imidazoleacetic acid (tele-MIAA) accounts for approximately 70–80% of metabolized histamine.[5] Tele-MIAA is excreted in urine, and urinary analysis therefore provides a non-invasive means to assess histamine-related activity. This approach has been used to investigate inflammatory and immune processes in various conditions, including viral infections. However, a key limitation of urine-based diagnostics is that analyte concentrations depend on several physiological factors, including hydration status, inflammation, glomerular filtration rate, kidney injury, and hormonal balance.[6] Consequently, metabolite concentrations must be normalized to endogenous reference compounds that reflect kidney function, such as creatinine or urea.

The urinary metabolites quantified in this study can be grouped according to their physiological and diagnostic relevance. The first group – the primary focus of this study – includes histamine metabolism and mast cell activation markers such as 1-methylhistamine (1MH), tele-MIAA, and 1-methyl-5-imidazoleacetic acid (pi-MIAA), which reflect histamine turnover and mast cell activity (Fig. 1a). For accurate quantification, it is essential to chromatographically separate

[a]Department of Forest Genetics and Plant Physiology, Swedish University of Agricultural Sciences, Umeå, Sweden. E-mail: ondrej.hodek@slu.se
[b]Swedish Metabolomics Centre, Umeå, Sweden
[c]Department of Clinical Microbiology, Umeå University, Umeå, Sweden
[d]The Laboratory for Molecular Medicine Sweden (MIMS), Umeå University, Sweden
[e]Department of Diagnostics and Intervention, Umeå University, Umeå, Sweden
[f]Department of Plant Physiology, Umeå University, Umeå, Sweden

the isomeric pair of pi- and tele-MIAA. Tele-MIAA is a well-established marker of histamine degradation, whereas the origin and biochemical pathway of its isomer, pi-MIAA, remain unclear. Pi-MIAA has been detected in several biological matrices, including urine, cerebrospinal fluid, and plasma,[7] but its physiological role and origin are still unknown.[8] Therefore, precise separation of these isomers is crucial for correctly assessing histamine degradation through tele-MIAA measurement.

The second group represents markers of muscle protein turnover, namely 1-methylhistidine (1MHis) and 3-methylhistidine (3MHis) (Fig. 1b). 1MHis arises from histidine methylation *via* dietary and endogenous processes, while 3MHis is produced during actin and myosin degradation. Elevated urinary excretion of 3MHis serves as a sensitive indicator of skeletal muscle protein catabolism. In inflammatory states, such as sepsis, it may also reflect changes in renal reabsorption and filtration functions and has been suggested as a marker of sepsis-acquired acute kidney injury.[11–14] A third group comprises metabolites involved in energy metabolism and methylation—guanidinoacetic acid (GAA), creatine, and creatinine (Fig. 1b). Measurement of these metabolites provides insight into cellular energy metabolism and methylation efficiency, as GAA is methylated to creatine using *S*-adenosylmethionine and creatine serves as a rapid ATP buffer in energy-demanding tissues. Clinically, their urinary or plasma levels are used to evaluate disorders of creatine metabolism, methylation imbalance, and renal function, and to normalize urinary metabolite concentrations in metabolomic studies.[15–17] Finally, nitrogen and purine metabolism markers—urea and uric acid—represent terminal products of amino acid and purine catabolism, respectively (Fig. 1b). Urea, the major nitrogenous end product of amino acid catabolism, serves as an indicator of nitrogen balance, hepatic urea-cycle activity, and renal concentrating capacity, and is routinely applied for normalization and assessment of metabolic load in urinary metabolomics.[18] Uric acid, the terminal purine metabolite, indicates purine turnover, oxidative stress, and renal excretory function.[19,20]

Together, these metabolites provide complementary insights into histamine metabolism, protein turnover, energy balance, nitrogen homeostasis as well as renal filtration and reabsorption – five physiological domains frequently perturbed during inflammation, infection, and metabolic stress.

Because the majority of the urine metabolites are small, polar, and ionic, capillary electrophoresis has traditionally been used for their quantification, including 1MHis, 3MHis, amino acids, GAA, creatine, creatinine, uric acid, and various inorganic ions.[21–26] However, conventional UV/VIS or CCD detection in capillary electrophoresis provides limited specificity and sensitivity. Even though the development of liquid chromatography coupled with mass spectrometry (LC-MS) has greatly improved analytical coverage, sensitivity, and selectivity for complex matrices such as urine, the reversed-phase LC still offers poor

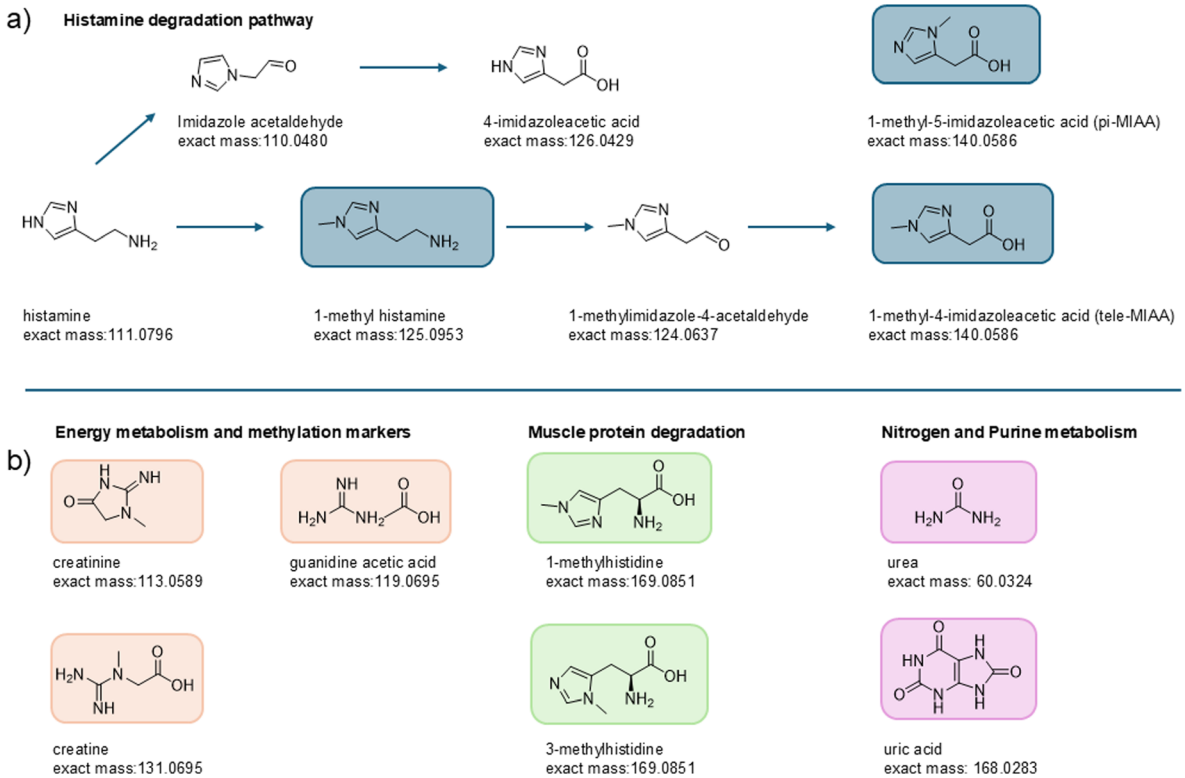

Fig. 1 Histamine metabolism pathways (a) and additional metabolites included in this study (b). Metabolites quantified by the HILIC-MS/MS method are highlighted. The HNMT pathway was targeted because it reflects systemic mast cell histamine turnover, whereas DAO mainly mediates intestinal degradation of dietary histamine. DAO, diamine oxidase; HNMT, histamine-*N*-methyltransferase; MAO-B, monoamine oxidase B; ALDH, aldehyde dehydrogenase.[9,10]

retention for small, highly polar compounds. For these analytes, ion-pair chromatography (IPC) and hydrophilic interaction liquid chromatography (HILIC) are more suitable alternatives.[5,27,28] While IPC requires charged reagents that can suppress ionization and contaminate chromatographic systems, HILIC allows efficient retention and separation of polar urinary metabolites such as urea, uric acid, creatinine, and histamine derivatives.

Several studies have used HILIC for quantifying histamine and its degradation metabolites in urine[29] and cerebrospinal fluid.[30] However, neither study included both pi- and tele-MIAA, which may substantially limit interpretation of MIAA quantification results.

Baseline separation of pi- and tele-MIAA was achieved in a study, where an IPC was used, though this method introduced several drawbacks.[31] Ion-pairing chromatography requires fluorinated carboxylic acids that adsorb onto steel and PEEK tubing, necessitating extensive cleaning of the LC/MS system. When operating in negative ESI mode, residual compounds can produce background ions if not properly removed. Furthermore, IPC methods require long equilibration times, reducing analytical throughput.

To date, no analytical method has provided simultaneous, rapid quantification of all these urinary metabolites. Therefore, in this study we developed, optimized, and validated a hydrophilic interaction liquid chromatography–tandem mass spectrometry (HILIC-MS/MS) method. The method enables precise quantification of ten clinically relevant urinary metabolites—urea, creatinine, 1MH, uric acid, pi-MIAA, tele-MIAA, creatine, GAA, 3MHis, and 1MHis—with baseline separation of isomeric compounds (1MHis/3MHis and tele-MIAA/pi-MIAA) within seven minutes (sample-to-sample). This analytical platform was applied to urine samples from COVID-19 patients, revealing distinct metabolite profiles in individuals with mild and severe disease compared to healthy controls.

Material and methods

Chemicals and reagents

LC-MS grade acetonitrile, ammonium formate, and formic acid were purchased from Sigma-Aldrich (MO, USA). Deionized water was supplied by MilliQ device from Merck-Millipore (MA, USA). Analytical standards of 1-methyl-L-histidine (≥98.0%), 3-methyl-L-histidine (≥98.0%), 1-methylhistamine (≥98.0%), guanidinoacetic acid (99%), uric acid (≥99%), urea (≥98.5%), urea-$^{15}N_2$ (99%) were purchased from Sigma-Aldrich (MO, USA). Creatinine-D3 (98%) and creatine-D3 (97%) were purchased from Cambridge Isotope Laboratories (MA, USA). 1-Methyl-L-histidine-D3 and uric acid-$^{15}N_2$ were purchased from MedChemExpress (NJ, USA). 2-(1-Methyl-1*H*-imidazol-5-yl)acetic acid (pi-MIAA) was purchased from BenchChem (TX, USA) and 1-methyl-4-imidazoleacetic acid (tele-MIAA) was purchased from Larodan (Sweden).

LC-MS conditions

The urinary metabolites were separated and quantified by using an LC-MS/MS system consisting of an Agilent 1290 UPLC connected to an Agilent 6495D triple quadrupole (Agilent, CA, USA). The separation was achieved by injecting 3 μL of a sample to a BEH amide column (30 × 2.1 mm, 1.7 μm, Waters, MA, USA). The mobile phase consisted of 10 mM ammonium fomate of pH 3.0 (adjusted with formic acid) in (A) water and in (B) acetonitrile/water 90/10 (v/v). The mobile phase was delivered on column by a flow rate of 0.6 mL min^{-1} with the following gradient: 0.0 min (99% B), 1.5 min (99% B), 3.0 min (30% B), 4.0 min (30% B), 4.1 min (99% B), 7.0 min (99% B). Column and autosampler were thermostated at 40 °C and 4 °C, respectively. Analytes were ionized in an electrospray ion source operated both in positive and negative modes. The source and gas parameters were set as follows: ion spray voltage −3.5 kV in negative and +4.0 kV in positive mode, gas temperature 150 °C, drying gas flow 11 L min^{-1}, nebulizer pressure 20 psi, sheath gas temperature 325 °C, sheath gas flow 12 L min^{-1}, fragmentor 166 V.

Multiple reaction monitoring (MRM) transitions of the urinary metabolites were optimized by using Agilent MassHunter Optimizer and MRM transitions were monitored in dynamic MRM mode during an analytical run. The LC-MS data was processed by using the Agilent MassHunter Qualitative 12.0.430.0 and QQQ quantitative analysis version B.12.0.893.1 (Agilent Technologies Inc., Santa Clara, CA, USA).

Preparation of standard solutions

For optimization and calibration purposes, the analytical standards were separately dissolved in deionized water to form 5 mg mL^{-1} solutions, with exception of uric acid that was dissolved in 1 mM aqueous sodium hydroxide. Afterwards, the stock solutions were diluted to the desired concentration with acetonitrile/water 80/20 (v/v). All the stock and working solutions were kept at −20 °C.

Sample preparation

The human urine samples used for validation were obtained from healthy adults with age between 20 and 73 years. The samples were frozen at −80 °C within 4 hours after sampling; prior to the analysis they were thawed at room temperature, vortex mixed, and 10 μL of urine was diluted 150× with 80% acetonitrile containing the internal standards (1 μM creatine-D_3, 1 μM 1-methyl-histamine-D_3, 1 μM 1-methyl-histidine-D_3, 1 μM 3-methyl-histidine-D_3). For quantification of the most abundant metabolites – creatinine, urea, uric acid – the 150× diluted urine was further diluted 40-fold with 80% acetonitrile containing internal standards of 10 μM creatinine-D_3, 10 μM urea-$^{15}N_2$, and 10 μM uric acid-$^{15}N_2$. Finally, 3 μL of each urine sample was injected on the analytical column (Fig. S1).

Clinical sample

All urine samples were taken with informed consent of all participants. Urine samples from patients with mild (n = 10) and severe (n = 10) COVID-19 were obtained from the prospective, observational cohort study CoVUm (https://clinicaltrials.gov identifier: NCT04368013) and used for further clinical validation of the method. Mild disease was defined as not requiring respiratory support or supplemental

oxygen, while severe disease was characterized by the need for high-flow nasal oxygen, non-invasive, or invasive mechanical ventilation. Patients were matched by age and sex. The study was approved by the Swedish Ethical Review Authority, Uppsala (DNR 2020-01557). Sample preparation was performed as described above. Concentrations were normalized to urinary creatinine levels, and differences between groups were analyzed by Kruskal–Wallis test followed by Dunn's *post hoc* multiple comparisons. The p-value of <0.05 was considered significant.

Method validation

The method for quantification of urinary metabolites on BEH amide column was validated through evaluation of parameters such as limit of detection (LOD), limit of quantification (LOQ), carry-over, linearity, matrix effects, accuracy, precision, and repeatability.

Sensitivity of the method was characterized by the LOD and LOQ values that were determined as a concentration corresponding to a signal-to-noise ratio (S/N) of 3 and 10, respectively.

Carry-over was assessed in a blank solvent injected on column after the analysis of the calibration solution of the highest concentration.

Linearity of the method was evaluated through 16-point linear regression model yielding the calibration curves constructed by using isotopically labelled standards for most analytes.

Matrix effects were assessed by spiking standard solutions into the diluted urine samples. The samples were spiked at three concentration levels – 0.5, 1, and 10 μM. The matrix effects were assessed based on comparison of the slope of the calibration curve with the slope of the curve constructed from the spiked samples according to the following equation:

$$\mathrm{ME} = 100 - \left(\frac{S - U}{S} \times 100\right)$$

where ME represents matrix effect (%), S is a slope of calibration curve constructed with neat standards, U is a slope of calibration curve constructed with standards spiked in a pooled urine sample.

Accuracy of quantitation was evaluated through the analysis of a real sample and the same sample spiked with standard solution (0.5, 1, and 10 μM standard addition); eventually, concentration in an original sample was subtracted from the total concentration in a spiked sample and accuracy was calculated as [(mean observed concentration)/(spiked concentration)] × 100%.

Precision was calculated as RSD for 6 repeated measurements of a real sample.

Repeatability in peak areas was determined as RSD of repeated measurements of one of the calibration solutions (1 μM, $n = 6$).

Results and discussion

Optimization of the LC-MS/MS conditions

Collision energy for each MRM transition of all urinary metabolites was optimized through flow injection analysis of a 10 μM standard solution (Table S1). Four MRM transitions were selected and tested in the on-column experiments. The two transitions with the highest signal-to-noise ratio were further used for analysis of real samples. Chromatographic conditions for separation of the urinary metabolites on the BEH amide column were optimized by using 10 mM ammonium formate of 3 different pH values – 3.0, 4.5, and 6.5. The mobile phase A consisted of pure aqueous 10 mM buffer, and the mobile phase B contained buffer mixed with acetonitrile so that the final solvent yielded 10 mM ammonium formate in 90% acetonitrile. The pH of mobile phase affected mainly retention of acidic compounds containing carboxylic group in their structure, namely tele-MIAA, pi-MIAA, GAA, 1MHis, and 3MHis. The buffer of pH 3 improved (i) the S/N through improved peak shapes while maintaining the same noise level, and (ii) separation for all metabolites, especially the isomeric 1MHis and 3MHis (Fig. 2).

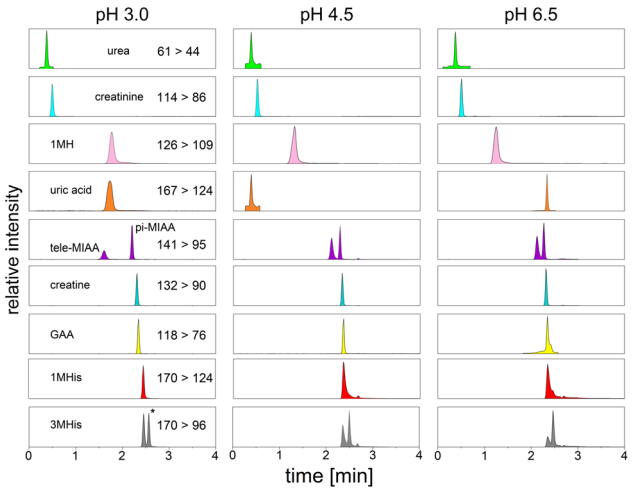

Fig. 2 Extracted ion chromatograms of the urinary metabolites and comparison of their retention and separation under different pH of the mobile phase.

In contrast with reversed-phase chromatography (RPLC), the HILIC mode is more susceptible to composition of the sample diluent. Significant amounts of water in the injected sample might lead to disturbance of the partitioning between organic and aqueous phase adsorbed on the stationary phase, thus resulting in peak splitting or tailing.[10,32] Therefore, various percentages of acetonitrile in the injected samples were evaluated in range from 50% up to 90% of acetonitrile in water. The amount of acetonitrile in an injected sample affected mainly retention of uric acid, tele-MIAA, and pi-MIAA. By comparing the FWHM values for all peaks, it became apparent that 80% and 90% acetonitrile in water provided very similar peak widths for all compounds (Fig. 3). As too high content of organic solvent in sample might affect solubility of very polar metabolites, 80% acetonitrile was used as the final diluent.

Method validation

The method showed highest sensitivity for creatinine with LOD and LOQ of 0.1 nM and 0.7 nM, respectively. On contrary, uric acid exhibited the lowest sensitivity with LOD and LOQ of

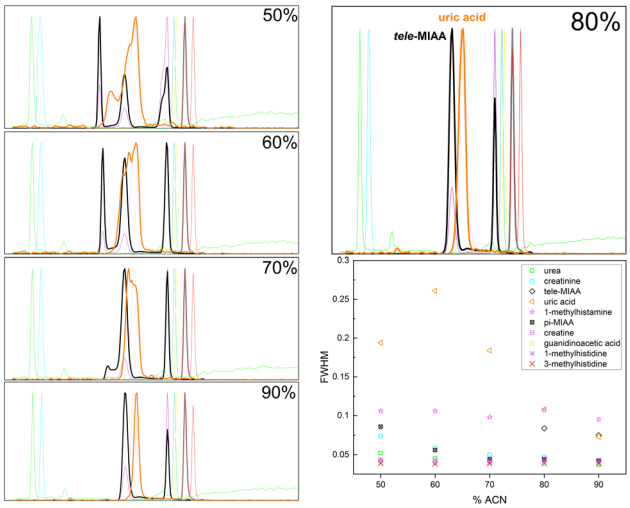

Fig. 3 The effect of acetonitrile as a sample diluent on the peak shapes of the urinary metabolites, % of acetonitrile in water (v/v).

200 nM and 500 nM, respectively, as a result of poor ionization of uric acid.

Carry-over assessment showed that there is no significant carry-over (less than 0.22%) from samples with high concentration levels of urinary metabolites.

Linearity of the method was acceptable with coefficients of determination (R^2) higher than 0.995 for the urinary metabolites quantified with isotopically labeled internal standard (IS). The calibration for tele-MIAA and pi-MIAA showed worse linearity – higher than 0.9648 – mainly because of the fact that IS for these compounds were not available (Table S2).

Matrix effects were evaluated in spiked urine sample. As the samples were diluted 150× and 6000×, respectively, the matrix effects were assessed at the corresponding dilution levels. Despite the large dilution, matrix effects reached significant values for most compounds like creatinine, 1-methylhistamine, tele-MIAA, creatine, and pi-MIAA with exception of 3MHis and uric acid whose signal was increased through ion enhancement effect.

Accuracy for all urinary metabolites found in human urine was in the acceptable range of 100 ± 15% at all three spiked levels. Accuracy for the most abundant metabolites (creatinine, urea, uric acid) was evaluated only at the highest spiked level (Table 1).

Precision was in acceptable range not exceeding RSD of 15%.

Targeted analysis of human urine from healthy individuals

In total, 13 samples were analyzed using the described methodology. All tested metabolites were found and quantified in all samples and their concentrations were normalized to urinary

Table 1 Accuracy and precision evaluated in samples of human urine. Matrix effects measured in spiked urine with matrix effects after normalization to internal standard in brackets

		Accuracy [%]			
Metabolite	Matrix effect [%]	0.5 μM	1 μM	10 μM	Precision [%]
1-Methylhistamine	23.2 (6.5)	114.1	112.3	91.0	0.3
Tele-MIAA	17.8	102.8	111.7	98.4	3.4
Pi-MIAA	14.8	94.5	101.9	100.8	1.8
Creatine	15.1 (−0.3)	102.6	101.5	97.8	0.8
Guanidineacetic acid	11.6	90.5	93.3	92.6	0.7
1-Methylhistidine	0.5 (−9.0)	113.5	107.4	111.2	1.4
3-Methylhistidine	−19.2 (0.7)	97.7	107.7	101.3	2.7
Urea	0.6 (2.6)	—	—	98.8	5.5
Uric acid	−10.8 (6.0)	—	—	95.2	1.5
Creatinine	26.6 (9.0)	—	—	93.4	0.7

Table 2 Concentration of urinary metabolites in normal human urine compared with reference values

Metabolite	Concentration in urine per 1 mmol creatinine[a] $n = 13$	Normal concentration in adults per 1 mmol creatinine[b]
1-Methylhistamine	72.1 ± 9.7 nM	32.0–130.0 nM
Tele-MIAA	1.6 ± 0.3 μM	1.3–2.3 μM
Pi-MIAA	3.5 ± 2.0 μM	1.1–8.3 μM
Creatine	34.6 ± 34.4 μM	11.3–113 μM
Guanidineacetic acid	75.1 ± 21.5 μM	7.7–89.0 μM
1-Methylhistidine	26.9 ± 2.9 μM	2.6–46.1 μM
3-Methylhistidine	77.0 ± 70.1 μM	5.4–69.3 μM
Urea	21.1 ± 4.3 mM	6.3–55.0 mM
Uric acid	366.6 ± 155.7 μM	23.8–543.0 μM
Creatinine	10.0 ± 3.6 mM	0.5–35.0 mM

[a] Average concentration ± confidence interval at a confidence level $\alpha = 0.95$. [b] HMDB database.

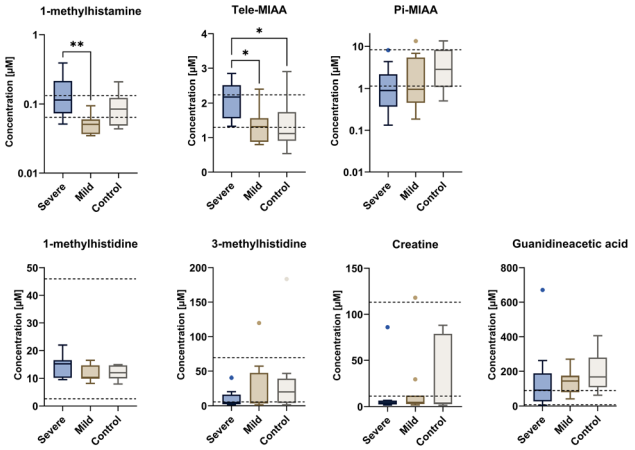

Fig. 4 Urinary histamine metabolites during acute COVID-19, stratified by initial disease severity in concentrations normalized to 1 mM creatinine. Data from severe (n = 10) and mild (n = 10) COVID-19 cases, as well as controls (n = 10), are depicted. Dashed horizontal lines indicate reference ranges for the reported normal concentrations in adults. P-Values were calculated using the Kruskal–Wallis test followed by Dunn's *post hoc* multiple comparisons test.

creatinine in order to account for variation in the rate of urine production.[32,33] The concentrations determined with the developed method suggest that 1-methylhistamine represents the least abundant metabolite with an average concentration of 72.1 nM per 1 mmol creatinine, whereas urea and uric acid were found in the highest concentrations. The concentrations of all metabolites found by using the developed method correspond with the reference range of normal concentrations quantified in healthy adults from the Human Metabolome Database (HMDB) (Table 2).[33]

Concentrations of histamine metabolites are shifted in acute COVID-19 compared to healthy controls

Notably, 1-methylhistamine levels were significantly elevated in severe COVID-19 cases relative to mild patients, exceeding reported normal adult values (Fig. 4). Accordingly, the downstream metabolite of 1-methylhistamine – tele-MIAA – was significantly elevated in severe cases. On contrary pi-MIAA, the metabolite of unknown origin decreased in mild and severe cases compared to controls. Similarly, 3-methylhistidine, creatine, and guanidineacetic acid were lower than the control group, although without statistical significance. Taken together, high levels of 1-methylhistamine and tele-MIAA in severe group indicate elevated histamine activity in acute COVID-19. While the number of clinical samples were few in this pilot study, our findings point towards interesting metabolic effects in acute COVID-19.

Conclusions

In this study, a fast and sensitive HILIC-MS/MS method was developed and validated for quantification of 10 metabolites in human urine, namely urea, creatinine, uric acid, 1-methylhistamine, 1-methyl-4-imidazoleacetic acid, creatine, guanidinoacetic acid, 1-methylhistidine, and 3-methylhistidine. As all quantified metabolites contain ionizable functional groups, the pH optimization of the buffered mobile phase was necessary to obtain good separation efficiency, which lead to baseline separation of isomeric pairs at pH 3.0. Tandem mass spectrometry in the MRM mode was used for detection, which enabled high specificity and sensitivity determined as LOQ that ranged from 0.7 nM for creatinine to 500 nM for uric acid as the metabolite with lowest sensitivity. The developed method enables high-throughput analysis of urine samples since it requires no derivatization step, and the separation is achieved only in 7 minutes. We applied the method to a small pilot cohort of acute COVID-19 patients (n = 20). We detected important differences in compound concentrations from healthy controls, indicating increased histamine activity and decrease in creatine synthesis from guanidine acetic acid, which might have clinical implications in explaining acute COVID-19 symptomatology.

Author contributions

Ondrej Hodek – conceptualization, investigation, methodology, validation, visualization, writing – original draft, writing – review & editing. Anna Edman – methodology. Christoffer Granvik – methodology, investigation, writing – original draft. Alicia Lind – investigation, writing – original draft. Anna K. Överby – investigation, writing – original draft. Mareike Gutensohn – methodology. Annika I. Johansson – resources, supervision, funding acquisition, writing – original draft, writing – review & editing.

Conflicts of interest

The authors declare that they have no conflict of interest.

Data availability

Raw data have been submitted to Metabolights and can be accessed at: https://www.ebi.ac.uk/metabolights/MTBLS13986. Additional data supporting this article have been included as part of the supplementary information (SI). Supplementary information is available. See DOI: https://doi.org/10.1039/d6ay00400h.

Acknowledgements

This work was supported by Knut and Alice Wallenberg Foundation (grant number KAW2018.0094 and KAW2014.0279), and Swedish University of Agricultural Sciences. Swedish Metabolomics Centre is also acknowledged for the technical support and Marie Lindgren for sample handling. Region Västerbotten grant number (RV-1014288, RV-996222 and RV-982568 to AKÖ) and (RV-992412 and RV-1010665 to AL).

References

1 M. Krystel-Whittemore, K. N. Dileepan and J. G. Wood, *Front. Immunol.*, 2016, **6**, 1–12.
2 S. Gebremeskel, J. Schanin, K. M. Coyle, M. Butuci, T. Luu, E. C. Brock, A. L. Xu, A. L. Wong, J. Leung, W. Korver, R. D. Morin, R. P. Schleimer, B. S. Bochner and B. A. Youngblood, *Front. Immunol.*, 2021, **12**, 650331.
3 L. B. Weinstock, J. B. Brook, A. S. Walters, A. Goris, L. B. Afrin and G. J. Molderings, *Int. J. Infect. Dis.*, 2021, **112**, 217–226.
4 D. Voelker and T. Pongdee, *Curr. Opin. Allergy Clin. Immunol.*, 2025, **25**, 27–33.
5 G. Granerus, B. Lönnqvist and U. Wass, *Inflammation Res.*, 1999, **48**, 75–80.
6 S. S. Waikar, V. S. Sabbisetti and J. V. Bonventre, *Kidney Int.*, 2010, **78**, 486–494.
7 J. K. Khandelwal, L. B. Hough, B. Pazhenchevsky, A. M. Morrishow and J. P. Green, *J. Biol. Chem.*, 1982, **257**, 2815–2819.
8 G. D. Prell, J. K. Khandelwal, L. B. Hough and J. P. Green, *J. Neurochem.*, 1989, **52**, 561–567.
9 S. Sánchez-Pérez, R. Celorio-Sardà, M. T. Veciana-Nogués, M. L. Latorre-Moratalla, O. Comas-Basté and M. C. Vidal-Carou, *Front. Nutr.*, 2022, **9**, 973682.
10 A. Maršavelski, J. Mavri, R. Vianello and J. Stare, *Int. J. Mol. Sci.*, 2022, **23**, 1910.
11 M. Elia, A. Carter, S. Bacon, C. G. Winearls and R. Smith, *Br. Med. J.*, 1981, **282**, 351–354.
12 I. Sampsonidis, M. Marinaki, A. Pesiridou, H. Gika, G. Theodoridis, N. Siachos, G. Arsenos and S. Kalogiannis, *Separations*, 2023, **10**, 144.
13 X. B. Wang, P. F. Huang, Y. H. Luo, Y. Xin, Y. Li, L. F. Shen, Y. Q. Liu, Y. Zhou, Y. X. Zhang, Q. Q. Zhang, D. W. Wang, F. Y. Luan, W. T. Zhang, M. Y. Yuan, Y. H. Liu, F. Y. Liu, N. Zhang, J. Y. Wu, T. Wu, X. Wang, Y. P. Bai, M. Y. Zhao, C. S. Wang and K. J. Yu, *Ann. Intensive Care*, 2025, **15**, 69.
14 E. Williamson, H. Kato, K. A. Volterman, K. Suzuki and D. R. Moore, *Amino Acids*, 2023, **55**, 1285–1291.
15 D. D. Nedeljkovic and S. M. Ostojic, *Clin. Bioenerg.*, 2024, **1**, 2.
16 S. M. Ostojic and J. Jorga, *Food Sci. Nutr.*, 2023, **11**, 1606–1611.
17 Y. H. Su, *Mol. Metab.*, 2025, **100**, 102228.
18 I. D. Weiner, W. E. Mitch and J. M. Sands, *Clin. J. Am. Soc. Nephrol.*, 2015, **10**, 1444–1458.
19 Y. Asahina, Y. Sakaguchi, T. Oka, K. Hattori, T. Kawaoka, Y. Doi, R. Yamamoto, I. Matsui, M. Mizui, J. Y. Kaimori and Y. Isaka, *Sci. Rep.*, 2024, **14**, 5119.
20 A. L. Iglesias, M. B. Pardo, C. R. Magariños, S. Pértega, D. S. Castro, T. G. Falcón, A. Rodriguez-Carmona and M. P. Fontán, *PLoS One*, 2024, **19**, e0304105.
21 R. Ramautar, O. A. Mayboroda, R. J. E. Derks, C. van Nieuwkoop, J. T. van Dissel, G. W. Sornsen, A. M. Deelder and G. J. de Jong, *Electrophoresis*, 2008, **29**, 2714–2722.
22 J. Rodríguez, J. J. Berzas, G. Castañeda, N. Mora and M. J. Rodríguez, *Anal. Chim. Acta*, 2004, **521**, 53–59.
23 P. Tuma, E. Samcová and P. Balínová, *J. Chromatogr. B*, 2005, **821**, 53–59.
24 Q. J. Wan, P. Kubán, J. Tanyanyiwa, A. Rainelli and P. C. Hauser, *Anal. Chim. Acta*, 2004, **525**, 11–16.
25 S. Zhao, J. Wang, F. Ye and Y. M. Liu, *Anal. Biochem.*, 2008, **378**, 127–131.
26 A. Zinellu, S. Sotgia, E. Zinellu, R. Chessa, L. Deiana and C. Carru, *J. Sep. Sci.*, 2006, **29**, 704–708.
27 C. Auray-Blais, B. Maranda and P. Lavoie, *Clin. Chim. Acta*, 2014, **436**, 249–255.
28 T. Sakurai, T. Irii and K. Iwadate, *Leg. Med.*, 2022, **55**, 102011.
29 M. Nelis, L. Decraecker, G. Boeckxstaens, P. Augustijns and D. Cabooter, *Talanta*, 2020, **220**, 121328.
30 Y. H. Zhang, F. D. Tingley, E. Tseng, M. Tella, X. Yang, E. Groeber, J. H. Liu, W. L. Li, C. J. Schmidt and R. Steenwyk, *J. Chromatogr. B*, 2011, **879**, 2023–2033.
31 J. Kolmert, B. Forngren, J. Lindberg, J. Öhd, K. M. Åberg, G. Nilsson, T. Moritz and A. Nordström, *Anal. Bioanal. Chem.*, 2014, **406**, 1751–1762.
32 J. Ruta, S. Rudaz, D. V. McCalley, J. L. Veuthey and D. Guillarme, *J. Chromatogr. A*, 2010, **1217**, 8230–8240.
33 T. Sato, Y. Kawasaki, M. Maekawa, S. Takasaki, S. Shimada, K. Morozumi, M. Sato, N. Kawamorita, S. Yamashita, K. Mitsuzuka, N. Mano and A. Ito, *Cancer Sci.*, 2020, **111**, 2570–2578.